

Performance-reliability trade-offs in short range RF power amplifier design

S.M. Pazos^{a,b,*}, F.L. Aguirre^{a,b}, F. Palumbo^{a,b}, F. Silveira^c

^a Unidad de Investigación y Desarrollo de las Ingenierías, Facultad Regional Buenos Aires, Universidad Tecnológica Nacional (UIDI FRBA-UTN), Medrano 951 (C1179AAQ), Buenos Aires, Argentina

^b Consejo Nacional de Investigaciones Científicas y Técnicas, Godoy Cruz 2290 (1425), Buenos Aires, Argentina

^c IIE, Fac. de Ingeniería, Universidad de la República, J. Herrera y Reissig 565 (11300), Montevideo, Uruguay

ARTICLE INFO

Keywords:

Power amplifier
Breakdown
Hot carriers
Design

ABSTRACT

In this work, trade-offs between performance and reliability in CMOS RF power amplifiers at the design stage are studied. The impact of transistor sizing, amplifier class and on-chip matching network design are explored for a 130 nm technology and the implications of design decisions in transistor gate oxide reliability are discussed and projected. A strong trade-off is observed between efficiency and reliability, mainly for different on-chip output matching architectures. A comparison between two example designs is performed via SPICE simulations that include reliability models and the effects of aging on the stress conditions of each amplifier.

1. Introduction

Short range RF Complementary Metal Oxide Semiconductor (CMOS) transmitters are flourishing in the current Internet of Things (IoT) paradigm for a wide range of applications including health monitoring [1]. In this scenario, critical applications involving this kind of circuits require a conscientious evaluation of reliability at a design stage, exploring trade-offs between performance aspects and expected reliability.

Transistor level reliability hazards have been widely studied to ensure a suitable working lifetime for products along the CMOS technology roadmap. Constant downscaling and increasing electric field in transistors made of time dependent dielectric breakdown (TDDB) [2] and Hot Carrier Injection (HCI) [3] a severe threat to device oxide reliability. But a majority of this research has been focused at the product level for, mostly, digital devices with very large scale of integration. Nevertheless, many efforts have been carried on so far to take reliability models into account to predict and implement on-chip strategies for reliability in RF circuits [4–7], but usually centred on analysis or simulation of a given design instead of incorporating the reliability aspect into a design space or architecture exploration.

In this work, we focus on class A-to-C power amplifiers (PAs) working at 2.455 GHz, fully integrated in a 130 nm RF CMOS technology. We propose a design stage exploration of reliability in terms of the matching resistance at the output, taking into account the trade-offs present during matching network design. TDDB and HCI effects are

introduced in the design exploration as the two main reliability hazards for PAs. To evaluate the design approach, a simulation study is performed on different PA designs in SPICE, each with a different output matching network topology, and the trade-offs between reliability and circuit performance are discussed. The remainder of the work is organized as follows: Section 4 revisits the TDDB and HCI models and summarizes the approach applied in this work; Section 5 discusses a design exploration of the trade-offs in PA design taking into account reliability indicators; Section 4 shows the comparative results between PA designs based in reliability aware SPICE simulations; finally, Section 5 draws the conclusions.

2. Transistor reliability models

2.1. Time dependent dielectric breakdown

TDDB is a stochastic phenomenon that has been modelled through percolation theory: the applied electric field and the leakage current through the gate oxide contribute to the build-up of defects until a percolation path is created spanning the oxide, forming a conductive path between the channel and the gate contact. The failure rate is characterized by Weibull statistics and strong power law or exponential voltage acceleration of the time to breakdown [2]. In this framework, circuit modelling of the transistor under Soft, Progressive and Hard Breakdown (SBD, PBD and HBD respectively) has been performed through resistors representing the conductivity of the percolation path

* Corresponding author at: Unidad de Investigación y Desarrollo de las Ingenierías, Facultad Regional Buenos Aires, Universidad Tecnológica Nacional (UIDI FRBA-UTN), Medrano 951 (C1179AAQ), Buenos Aires, Argentina

E-mail address: spazos@frba.utn.edu.ar (S.M. Pazos).

Table 1
Summary of degradation models.^a

$t_{63} = \frac{T \cdot t_0}{\left(\frac{A_{ox}}{A_{ref}}\right)^{1/\beta} \int_0^T V_{G(S/D)}(\tau)^m d\tau}$		
$t_{100ppm} = t_{63}(-\ln(1 - 10^{-4}))^{1/\beta}$		
$\mu_{HCl} = \left(\frac{\mu_0}{\left(\frac{\Delta V_{thHCl} C_{ox}}{q \alpha_{HCl}} + 1\right)^{m_\mu}}\right)$		
$\Delta V_{thHCl} = \frac{q}{C_{ox}} K_{HCl} \sqrt{Q_i} e^{\frac{E_{ox}}{E_0}} e^{-\frac{\Phi_{it}}{q \lambda E_m}} t^{n_{HCl}}$		
$E_m = \frac{V_{ds} - V_{dssat}}{l}$		
$E_{ox} = \frac{V_{gs} - V_{th}}{t_{ox}}$		
$\beta = 1.5$	$m = 11$	$t_0[s] = 6 \times 10^{11}$
$K_{HCl} [nm \cdot \sqrt{C}] = 1.7 \times 10^8$		$\alpha_{HCl} = 5$
$E_0[V/nm] = 0.8$	$\lambda[nm] = 7.8$	$n_{HCl} = 0.44$
$l[nm] = 34$	$m_\mu = 1.6$	$\Phi_{it}[eV] = 3.7$

^a Technology dependent parameters for TDDB models. Values are extracted from the literature: β is the Weibull slope [2], m is the voltage acceleration [2, 10], t_0 is the displacement of the t_{63} vs. VG curve fitted from [2] and references therein. Technology dependent parameters for HCI models. Values are extracted from the literature: K_{HCl} is a fitting parameter [5], α_{HCl} is a proportionality factor that depends on substrate doping [5], E_0 is HCI-driven defects activation energy [5], λ is the mean free path [9], n_{HCl} is the time acceleration factor, l is the pinch-off region approximate length [9], m_μ is the power law acceleration of mobility degradation and Φ_{it} is the minimum energy required to create a defect [9].

[8].

TDDB models characterize time to failure by a Weibull distribution with shape factor β for a technology with a voltage power acceleration factor m , which allows to extrapolate a reference time to failure (100 ppm failed parts in this work, t_{100ppm}). This acceleration factor was chosen to fit the projected lifetime of a 2.2 nm thick SiO₂ (as for the technology used in this work) [10]. It should be pointed out that m can take different values at accelerated degradation conditions due to the reduction of defect generation probability at low voltages, as shown by long term (2 years) experimental results [2]. Expressions 1 and 2 in Table 1 show the dependences with voltage and technology of the Weibull characteristic time t_{63} and the extrapolation to lower failure rates t_{100ppm} through the Weibull inverse function.

As per SBD and PBD, numerous models have been developed to represent the conduction through a nanometric percolation path that presents relatively high resistivity (from tens to thousands of k Ω) with a strong dependence on stress time and voltage [11]. However, the high resistivity of a SBD path has been shown to have negligible impact on PA operation [12]. This will be briefly discussed in the next section of this work.

After HBD, the final resistance of the BD path has been shown to range from a few to tens of k Ω with a strong dependence on the relative position of the path in the channel [8]. Under these conditions it is possible to adopt a single β to characterize TDDB for this particular circuit under test. As per the modelling of such breakdown paths in the circuit level, a common approach [6] is to place resistors connected between gate and source (R_{GS}) or gate and drain (R_{GD}) according to the region of the gate where the BD event is considered to take place. Multiple gate oxide breakdown events can be considered in order to accurately predict the degradation of a circuit with time [13], but it will be shown that the impact of such events is strongly dependent with the dominant degradation mechanism for a certain design and can be therefore pondered in a design stage before any simulation models are implemented.

2.2. Hot carrier injection

HCI is a degradation mechanism that has been mainly linked to

Si–H bond breaking [3], which is driven by the high electric fields in the channel (mainly in the vicinity of the drain). Channel carriers acquire sufficient energy from these fields to surpass the oxide-semiconductor barrier. The main consequence of energetic carriers in the channel is the injection of charge into the dielectric, causing an overall deviation in threshold voltage (ΔV_{thHCl}) and a reduction in the effective mobility (μ_{HCl}). Hence, this effect translates into time dependent parametric degradation of the device that has a strong impact on the RF performance both at the device and at the circuit level [3–7]. As an electric field-driven phenomenon, HCI has been widely characterized to have exponential dependence on drain and gate voltages (V_{DS} and V_{GS}), and to have a power law characteristic with time [9], as shown in Eqs. (3) to (6) in Table 1. Finally, although the effects of RF stress on the impact of TDDB and HCI on device performance has been reported in the literature, there is no general model to assess the impact of the RF stressing conditions on device reliability. It has been proposed in [16] that oxide degradation under RF stress conditions shows a correlation with RMS voltages. On the other hand, the quasistationary sum (QS) of DC signals has shown good agreement with experimental results in [14]. In this work, the latter approach [14] is adopted as it imposes a worst case scenario in terms of the degradation prediction of the circuit under study.

A summary of the models considered during design exploration and circuit simulation is shown in Table 1, along with the adopted values for the technology dependent parameters involved in each model. In these expressions, T stands for the period of the RF signal, t_0 is the displacement parameter of the t_{63} power law acceleration model, A_{ox} and A_{ref} are the device under test and reference areas for area scaling (where half the total Aox is assumed as a rough approximation for GS or GD breakdown). For HCI models, μ_0 is the mobility parameter of a fresh device, C_{ox} the oxide capacitance per unit area, q the electron charge, E_{ox} is the vertical electric field (due to V_{GS}), E_m is the lateral electric field. Model-specific parameters are defined in the footnote of Table 1. It should be pointed out that technological parameters are strongly dependent of technology node and fabrication process, therefore parameter spread can be expected for different manufacturers. In this work, typical parameter values for a 130 nm CMOS node were considered.

3. Design trade-offs for reliability in RF PA

3.1. Impact of BD path modeling on PA performance

Modelling of the BD path between gate and source or gate and drain can show very different sensitivities in terms of circuit performance. This can be explained by the impact of such resistors on the RF performance of the device. While RGD has a direct impact on the transducer gain, RGS impacts introducing an impedance mismatch at the input of the circuit, without any impact on the transducing characteristics. Therefore, same performance degradation of the PA is observed for slightly higher values of RGD than RGS, so RGD can be considered as a worst case from the point of view of its impact on reliability.

In terms of impedance, as the whole circuit operates at relatively low impedance values (tens of Ω), high valued resistive breakdown paths don't represent a hazard for performance of the PA. For the process used in this work, considerable degradation of PA performance is only observed for resistances < 2K Ω . Under this condition, for such low values of RGD and RGS required to observe a clear degradation of circuit performance, it is fairly accurate to only consider severe gate dielectric breakdown (i.e. HBD) in the reliability estimation of a PA.

3.2. Design exploration for reliability

The PA is a circuit block where high voltages and currents are handled, thus pushing reliability limits. RF PA design is most often a trade-off between linearity, area consumption and power efficiency at a

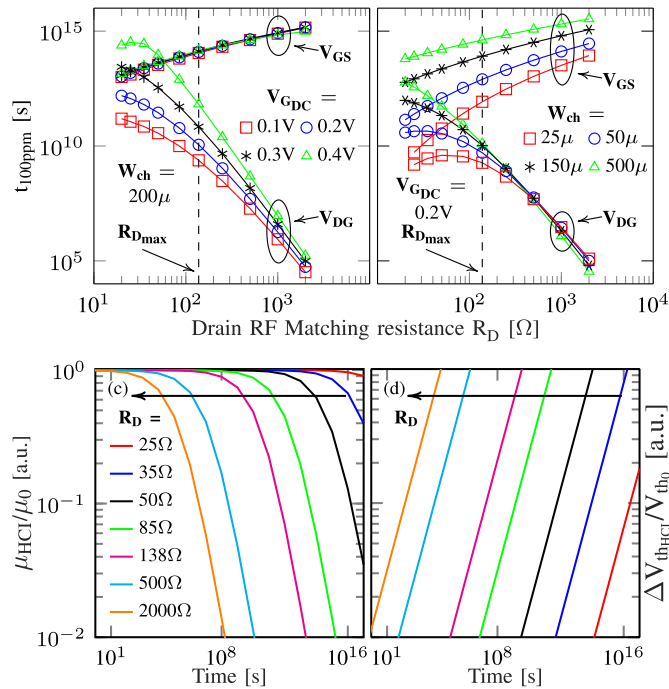


Fig. 1. Reliability indicators. (a) t_{100ppm} vs. R_D for different PA class and (b) impact of transistor sizing at constant V_{GDC} , in both cases considering V_{GS} and V_{DG} stress. (c) Relative μ_{HCl} and (d) ΔV_{thHCl} due to HCl.

fixed desired output power (P_{out}). A good approximation to optimal design can be achieved by a generalized design space evaluation [15] but bringing reliability to the table adds new degrees of freedom to take into account. Considering that the drain is operating at a high selectivity (Q_D), the fundamental component of the drain current ($id_{n,1}$) or voltage (vd_{rf}) should be such to obtain the desired output power, given by $P_{out} = vd_{rf}^2 / 2RD = id_{n,1}^2 \cdot R_D / 2$, neglecting for the moment the losses in the output matching network, being R_D the converted impedance towards the drain.

From a reliability perspective at constant P_{out} , higher RF resistance on the drain implies higher drain RF voltage and hence higher V_{Ddc} to ensure a V_{DSmin} that keeps the device in saturation. This is desirable for MOSFET efficiency η_{MOS} -calculated as $id_{n,1}(V_{Ddc} - V_{DSmin}) / (2Id_{DC} \cdot V_{Ddc})$ but larger lateral and vertical electric fields will result in a faster degradation. On the other hand, lower RF resistance on the drain results in a higher required drain current, which means a larger RF peak voltage at the gate of a transistor of a given size. This design perspective of reliability is summarized in Fig. 1a to 1d, where the main reliability indicators (t_{100ppm} , ΔV_{thHCl} and μ_{HCl}) are shown as a function of the R_D for different transistor size or gate DC bias on the considered RF CMOS 130 nm commercial process. The main feature observed in Fig. 1a is the fast drop on t_{100ppm} with R_D when considering drain-to-gate stress (V_{DG}) for a fixed transistor width of 200 μ m.

It should be pointed out that the vertical dashed line in the plot indicates the maximum value of R_D that ensures a peak V_D below the nominal for this technology (1.2V). Higher resistance values are considered, nonetheless, as oxide stress can be linked instead to the rms electric field [16] or the QS approach [14]. Another important characteristic is that under the QS assumption, for gate-to-drain stress, TDDB models are strongly dependent with the operating class of the amplifier, determined by the conduction angle θ_c which is defined by V_{GDC} and V_{GRF} . This is observed as for smaller θ_c (towards class C, lower V_{GDC} in Fig. 1a) t_{100ppm} is reduced at constant R_D due to higher drain-gate DC and RF peak stress. Fig. 1c and d show HCl degradation curves, observing a displacement of the μ_{HCl} and ΔV_{thHCl} towards longer times as R_D decreases, as expected at lower drain RF voltages.

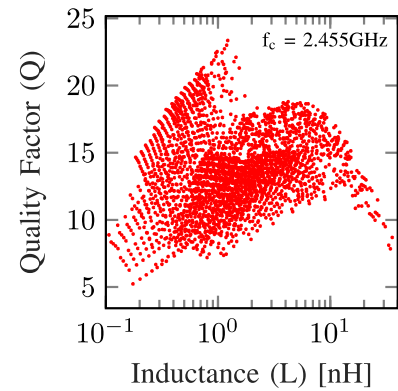


Fig. 2. Space of inductors in the 130 nm technology used in this work. Q vs. L is shown, where a maximum of 24 is observed for inductors around 1nH.

In addition to P_{out} specification, efficiency is a key parameter in PA design. Total efficiency is comprised by η_{MOS} and output matching network efficiency (η_{NW}), i.e. its insertion loss (IL), caused by real elements. In this regard, and for on-chip matching, inductors are the bottleneck in virtually every RF design due to their high losses and limited range of values. For the inductor space available in a given technology, only a handful of matching networks can be designed for a given R_D/R_L , each one resulting in different Q_D and IL.

The main limitation, as mentioned previously, is the limited inductor space for a given technology. This can be observed in Fig. 2, where inductor Q_0 vs. inductance (L) is represented in a scatter plot for the whole space of inductors in the technology being employed (scatter was slightly down sampled for clarity purposes). Clearly, highest Q values > 20 (lower loss) are limited to an inductance range between 400 pH and 1 nH, dropping rapidly for higher and lower L values. For a given R_D/R_L , these inductors are used to create a space of matching networks that comply with this impedance hop, but each with a different Q at the load and drain sides and different magnitudes for IL. Additionally, network topology is different for $R_D/R_L > 1$ or < 1 . Fig. 3a shows a PA with a generalized π -network for output matching. The capacitive or inductive nature of the series branch defines $R_D/R_L > 1$ or < 1 respectively.

Fig. 3b shows, for those networks that achieve a certain Q_D ($\sim 1\%$ tolerance), the one that has the lowest IL. It is now possible to directly observe the trade-off between impedance conversion (RL is 50 Ω in all cases), IL and operating Q_D . It is important to notice that a low Q_D value results in high harmonic content, rendering the high selectivity condition for PA design invalid, requiring specific analysis of the drain voltage waveforms for such condition to assess reliability. As general trend, highest efficiencies are obtained for $R_D/R_L > 1$ with an IL loss higher bound of around 2 dB but for low Q_D values. From the reliability perspective, for $R_D/R_L < 1$ and high Q_D , IL rapidly increases due to inductor losses in the series branch, highlighting a trade-off between reliability and efficiency. As a rule of thumb, considering a design for R_D lower than 20 Ω would imply such a drastic efficiency loss ($< 1/4$ from the ideal case) at an acceptable Q_D that the design would be virtually unemployable for a majority of applications. Nevertheless, it should be pointed out that this lower bound is technology dependent, and therefore it should be explored for each particular case.

4. Reliability simulations of PA design cases

Transistor degradation models [2, 8, 9, 13] were introduced into a Spectre RF simulation flow. The circuit is simulated under a periodic steady state (pss) for different elapsed times of continuous operation. In each time instant, the drain and gate voltage waveforms are obtained and used to calculate the degradation parameters to be introduced into the design and used for the simulation of the next time step. The general

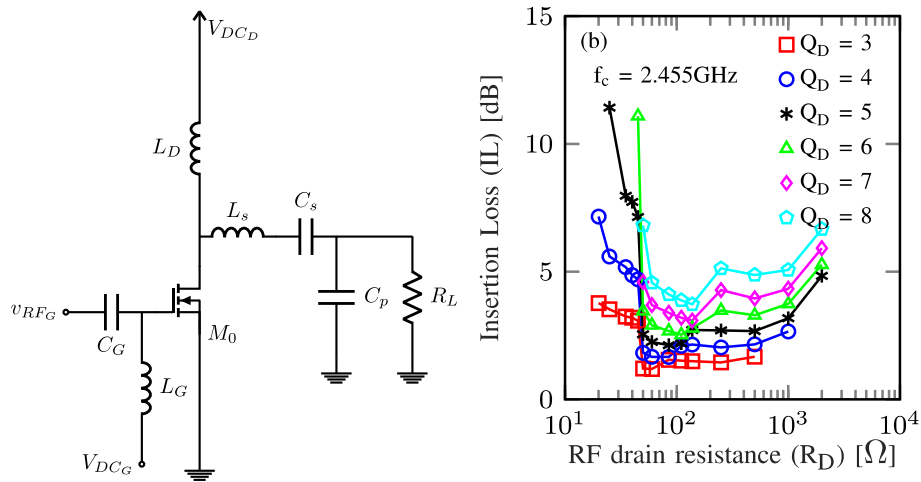


Fig. 3. Generalized topology of a single transistor PA. The plot (b) shows the insertion loss of the output network vs. the impedance conversion and the operating Q_D .

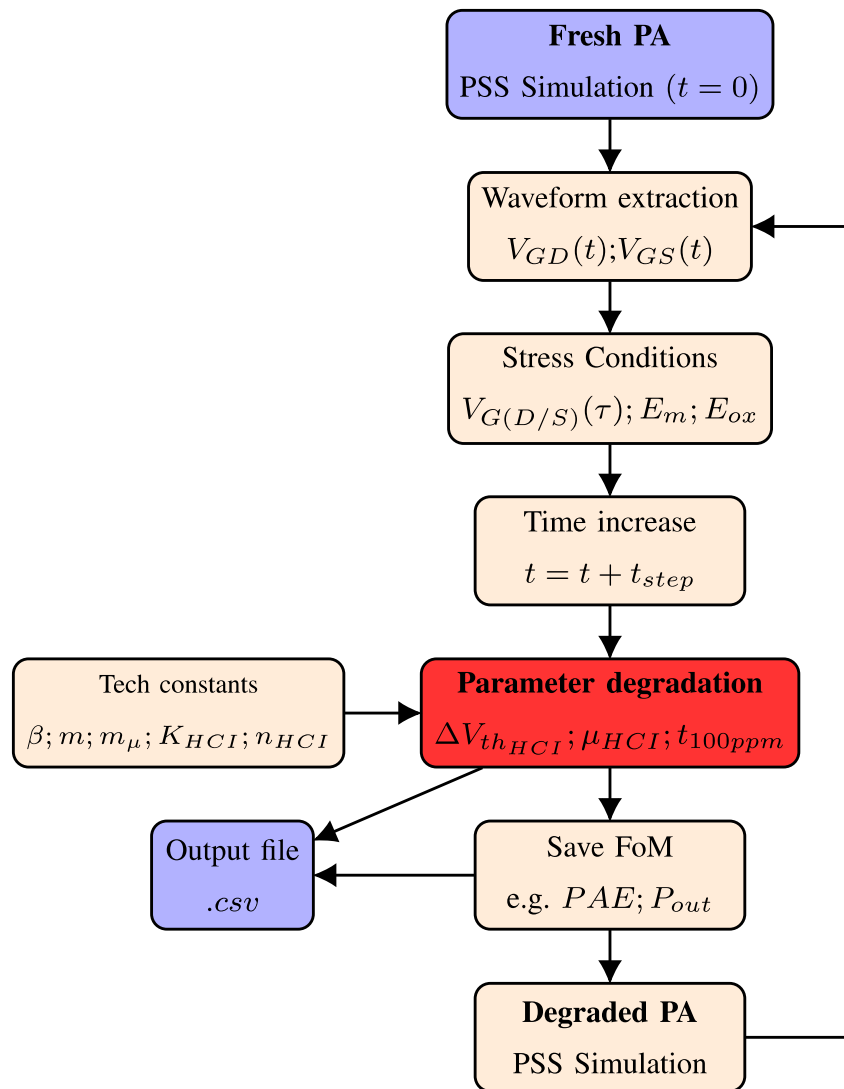


Fig. 4. Flow chart summarizing the used simulation script under Spectre RF for assessing PA degradation over time.

simulation procedure here described is represented in the flow chart of Fig. 4. It should be pointed out that, for these specific circuits, although TDDB parameters were calculated during simulations, the BD resistance model was not implemented for the circuits under test in this work due

to the negligible impact of TDDB in these designs. This will be discussed further along this section.

Two fully integrated 0 dBm P_{out} PA designs suitable for low power short range links were simulated, each with a different matching

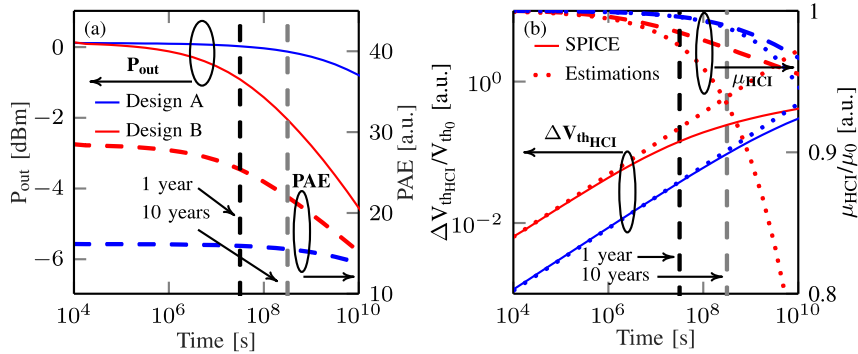


Fig. 5. SPICE simulation results for des. A ($R_D = 40 \Omega$) and des. B ($R_D = 85 \Omega$). (a) PAE and P_{out} evolution with time. (b) Comparison between the estimated parametric degradation at fresh condition (dotted) and the impact of updating stress conditions with time in SPICE (solid and dashed).

strategy at the drain: circuit A was designed to present $R_D = 40 \Omega$ while circuit B presents $R_D = 85 \Omega$. Drain DC voltage was afterwards fixed to maximize power added efficiency (PAE) and both circuits have identical V_{Gdc} and transistor sizing. Fig. 5 shows the summary of the simulation results for both circuits under test. P_{out} (solid) and PAE (dashed) evolution with time are shown in Fig. 5a, where design A shows a clear advantage on the parametric degradation when compared to design B: for a reference time, e.g. 10 years, circuit B shows a P_{out} reduction of > 2 dB while circuit A suffers a loss < 0.05 dB. The trade-off to this robustness is, as expected in the design stage, power efficiency: circuit A shows PAE around 15% while circuit B around 28%. Nevertheless, efficiency also degrades rapidly for circuit B, dropping 6% for the considered reference time while circuit A suffers an efficiency loss smaller than 1%. These simulations highlight the strong trade-off between design robustness and power efficiency of two different implementations of the same circuit.

It is important to point out the fact that, for this particular study, HCI degradation requires much shorter times to impact on circuit performance than the required time that, statistically, it would take 100 ppm circuits to experience gate oxide HBD (extrapolated from Weibull statistics). This is a consequence of the high extrapolated BD times for the referenced experimental data [10] to small transistor areas and low voltages, which yielded t_{100ppm} values in the order of 1×10^{13} seconds for the operating conditions of our circuits. Nevertheless, for different experimental TDDB data, the general variation of reliability indicators under projected design conditions would show the same trends as in Fig. 1, not affecting the design approach here presented. It would be required though, to take into account TDDB effects in the PA reliability simulation flow depicted in Fig. 4 if t_{100ppm} values are low enough.

Finally, another interesting issue is included in Fig. 5b, where the parameter values for μ_{HCl} and ΔV_{thHCl} are shown for both circuits as obtained from Spectre RF simulations (solid and dashed lines) and as estimated at the design stage considering the operation of the fresh circuit (dotted lines). Clearly, the design estimation shows much faster parametric degradation than the SPICE simulation results, highlighting the importance of updating the stress conditions over time for a precise assessment of reliability after a specific design has been chosen.

5. Conclusions

In this work, a design perspective for reliability of low power CMOS RF PAs is introduced. Results show a reliability enhancement for lower drain voltages at constant output power, but with a strong trade-off with matching network efficiency for on-chip implementations. This trade-off can be performed, at constant output power, by reducing the RF drain resistance. Finally, the importance of a SPICE implementation to simulate device lifetime was highlighted by the fact that circuit degradation changes the stressing conditions as well, and these should be

updated in time dependent reliability simulations to avoid underestimating circuit lifetime.

Acknowledgments

The research leading to this work was funded by the following institutions: in Argentina, UTN.BA under projects EIUTIBA4395TC, EIUTIBA4764TC and UTNI3856, CONICET under project PIP11220130100077CO and MINCyT under project PICT2013/1210; in Uruguay, Universidad De La República under article 57 and the 720 program.

References

- [1] Y.L. Zheng, X.R. Ding, C.C. Yan Poon, B.P. Lai Lo, H. Zhang, X.L. Zhou, G.Z. Yang, N. Zhao, Y.T. Zhang, Unobtrusive sensing and wearable devices for health informatics, *IEEE Trans. Biomed. Eng.* 61 (2014) 1538–1554.
- [2] J.H. Stathis, Reliability limits for the gate insulator in CMOS technology, *IBM J. Res. Dev.* 46 (2002) 265–286.
- [3] Y. Mammy Randriamihaja, A. Zaka, V. Huard, M. Rafik, D. Rideau, D. Roy, A. Bravaix, P. Palestri, Hot carrier degradation: from defect creation modeling to their impact on NMOS parameters, *Microelectron. Reliab.* 52 (2012) 2513–2520.
- [4] V. Huard, T. Quemerais, F. Cacho, L. Moquillon, S. Haendler, X. Federspiel, Design-in reliability approach for Hot Carrier injection modeling in the context of AMS/RF applications, 2011 Int. Reliab. Phys. Symp., IEEE, 2011(p. 5A.5.1-5A.5.7).
- [5] D. Chang, J.N. Kitchen, S. Kiaei, S. Ozev, In-field recovery of RF circuits from wearout based performance degradation, *IEEE Trans. Emerg. Top. Comput.* (2017) 1.
- [6] G.T. Sasse, M. Acar, F.G. Kuper, J. Schmitz, RF CMOS reliability simulations, *Microelectron. Reliab.* 48 (2008) 1581–1585.
- [7] J. Fritzin, T. Sundstrom, T. Johansson, A. Alvandpour, Reliability study of a low-voltage Class-E power amplifier in 130 nm CMOS, *Proc. 2010 IEEE Int. Symp. Circuits Syst.*, IEEE, 2010, pp. 1907–1910.
- [8] B. Kaczer, R. Degraeve, A. De Keersgieter, K. Van de Mierop, V. Simons, G. Groeseneken, Consistent model for short-channel nMOSFET after hard gate oxide breakdown, *IEEE Trans. Electron Devices* 49 (2002) 507–513.
- [9] Wenping Wang, V. Reddy, A.T. Krishnan, R. Vattikonda, S. Krishnan, Yu Cao, Compact modeling and simulation of circuit reliability for 65-nm CMOS technology, *IEEE Trans. Device Mater. Reliab.* 7 (2007) 509–517.
- [10] J.H. Stathis, D.J. DiMaria, Reliability projection for ultra-thin oxides at low voltage, *Int. Electron Devices Meet.* 1998. Tech. Dig. (Cat. No.98CH36217), IEEE, 1998, pp. 167–170.
- [11] S. Lombardo, J.H. Stathis, B.P. Linder, K.L. Pey, F. Palumbo, C.H. Tung, Dielectric breakdown mechanisms in gate oxides, *J. Appl. Phys.* 98 (2005) 121301.
- [12] K. Kutty, J.-S. Yuan, S. Chen, Evaluation of gate oxide breakdown effect on cascode class E power amplifier performance, *Microelectron. Reliab.* 51 (2011) 1302–1308.
- [13] J. Suñé, E.Y. Wu, W.L. Lai, Successive oxide breakdown statistics: correlation effects, reliability methodologies, and their limits, *IEEE Trans. Electron Devices* 51 (2004) 1584–1592.
- [14] A.J. Scholten, D. Stephens, G.D.J. Smit, G.T. Sasse, J. Bisschop, The relation between degradation under DC and RF stress conditions, *IEEE Trans. Electron Devices* 58 (2011) 2721–2728.
- [15] N. Barabino, R. Fiorelli, F. Silveira, Efficiency based design flow for fully-integrated class C RF power amplifiers in nanometric CMOS, *Proc. 2010 IEEE Int. Symp. Circuits Syst.*, IEEE, 2010, pp. 2223–2226.
- [16] L. Larcher, D. Sanzogni, R. Brama, A. Mazzanti, F. Svelto, Oxide breakdown after RF stress: experimental analysis and effects on power amplifier operation, 2006 IEEE Int. Reliab. Phys. Symp. Proc., IEEE, 2006, pp. 283–288.